GEOPHYSICAL RESEARCH LETTERS, VOL. 19, NO. 22, PAGES 2267-2270, NOVEMBER 20, 1992

INITIAL INVESTIGATION OF THE LANDERS, CALIFORNIA, EARTHQUAKE OF 28 JUNE 1992 USING TERRAscope

Hiroo Kanamori, Hong-Kie Thio, Doug Dreger, and Egill Hauksson

Seismological Laboratory, California Institute of Technology

Tom Heaton

U. S. Geological Survey, Pasadena, CA

Abstract. The 1992 Landers earthquake (M_S=7.5, M_W=7.3) was recorded at six TERRAscope stations in southern California. Peak accelerations ranged from 0.16 g at SVD (Δ=63 km) to 0.0092 g at ISA (Δ=245 km), decreasing with distance away from the fault zone. The peak velocity showed a different pattern reflecting the rupture directivity from south to north. The largest peak velocity, 19 cm/sec, was observed at GSC (Δ=125 km). Moment tensor inversion of long-period surface waves yielded a mechanism with M_0=1.1x10^{27} dyne-cm (M_W=7.3), dip=74°, rake=-176°, and strike=340°. Inversion of teleseismic *P* and *S* waves revealed two distinct sub-events of 6 and 8 sec duration and about 10 sec apart. The source parameters for the first and second events are: M_0=1.9x10^{26} dyne-cm, dip=83°, rake=179°, strike=359°; and M_0=6.1x10^{26} dyne-cm, dip=87°, rake=178°, strike=333°, respectively. The radiated wave energy, E_S, was estimated as 4.3x10^{23} ergs. The ratio E_S/M_0=3.9x10^{-4} corresponds to a stress drop of 280 bars, and suggests that the Landers earthquake belongs to the group of high stress drop earthquakes, and occurred on a fault with a long recurrence time. The rupture directivity can be seen clearly in the records from PFO (Δ=68 km) located to the south and GSC located to the north of the epicenter. The maximum displacement at PFO is only 13% of that at GSC despite the shorter epicentral distance to PFO than to GSC. The slip distribution determined with the empirical Green's function method indicates that the Landers earthquake consists of two distinct sub-events about 30 km apart, with the second sub-event to the north being about twice as large as the first one. This slip distribution is consistent with the teleseismic data and the surface offsets mapped in the field.

Introduction

The Landers Earthquake (M_S=7.5, M_W=7.3, June 28, 1992, 11h57m34s GMT, 34.20°N, 116.44°W) was recorded by the six TERRAscope stations (for TERRAscope, see Kanamori *et al.*, 1991). Figure 1 shows the TERRAscope stations, the mainshock epicenter and the rupture zone depicted by the aftershocks. It is the largest earthquake that has occurred in the middle of TERRAscope. Because the TERRAscope stations are located in a distance range of 63 to 303 km, they provided a unique data set for determining the source characteristics which are needed for various post-earthquake studies such as field mapping of surface breaks, strong-motion estimation, geodetic survey (especially GPS), and computation of stress changes on the adjacent faults.

The near real-time availability of strong-motion parameters from TERRAscope was important for rapid hazard assessment in southern California following the Landers earthquake. The spatial distribution of strong-motion parameters such as the peak acceleration and velocity was available within three hours. In the case of the 1992 Landers earthquake, no specific action was taken following the determination of the spatial distribution of strong ground shaking because it occurred in a sparsely populated part of the eastern Mojave desert and did not cause as much damage as a similar sized event located near a major population center could have. Nonetheless the experience gained in the Landers earthquake will be important for guiding rapid data analysis following future potential damaging earthquakes.

Paper number 92GL02320
0094-8534/92/92GL-02320$03.00

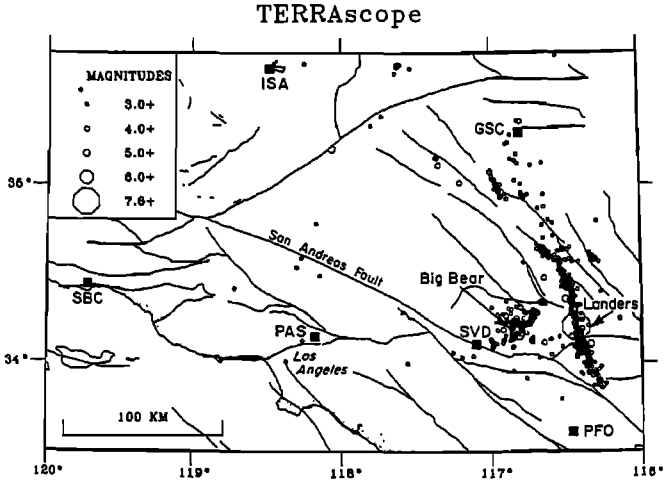

Fig. 1. TERRAscope stations, the mainshock of the 1992 Landers earthquake, and the aftershocks of M≥3.0 from 28 June to 30 September 1992.

The near real-time determination of the fault geometry, seismic moment and radiated energy can be used to estimate stress changes caused by this earthquake which in turn can be used to estimate the event's potential for triggering further earthquake activity on the adjacent faults such as the San Andreas fault. The Landers earthquake caused changes in both normal and shear stress on the San Andreas fault.

The Landers earthquake caused a spectacular surface break extending over 70 km with offset as large as 6.5 m (Landers Earthquake Response Team, 1992). The wide dynamic range of TERRAscope allowed us to determine the slip distribution along the fault. This slip distribution agreed well with the one mapped in the field.

Peak Accelerations and Velocities

The low-gain channels recorded the strong ground motions on scale at all the TERRAscope stations, while the surface wave portion of the very broadband (VBB) channels were clipped. (A minor timing error was found for station GSC, but it was later corrected using the *P*-wave arrival time, recorded independently by the Southern California Seismographic Network.). All of the low-gain and VBB data were retrieved

Table 1 Peak Acceleration and Velocity

Station	Δ_f(km)	ϕ(°)	a (Obs.)	a (C.)	v (Obs.)	v(C.)
PFO	59	182	4.5	7.3	4.6	9.3
GSC	45	344	5.8	10.4	19	14
SVD	59	258	16	7.3	10	9.3
PAS	151	268	3.2	1.7	8.3	2.2
ISA	169	311	0.92	1.4	3.2	1.7
SBC	258	276	1.0	0.50	3.0	0.60

Note: Δ_f is the distance to the nearest pont on the fault; ϕ is the azimuth; a (Obs.) is peak acceleration in % of g; a (C.) is computed peak acceleration; v (Obs.) is peak velocity in cm/sec; v (C.) is computed peak velocity.

from the stations within two hours. In contrast, strong-motion data from SMA-1 film recorders need to be retrieved from the field and developed. They are usually available after days or weeks.

Table 1 compares the observed peak accelerations and velocities with those computed for an M_w=7.3 event using the empirical relations of Joyner and Boore (1981). The recorded higher velocity at GSC to the north as compared to the relatively lower velocity at PFO to the south is probably caused by the south-to-north directivity, which is suggested by the spatial distribution of the mainshock and the immediate aftershocks (Hauksson *et al.*, 1992). The directivity appears more pronounced in velocity than acceleration, a fact which may have affected the spatial pattern of damage caused by this earthquake. The path to SVD is close to the San Andreas fault zone, which is probably responsible for the high acceleration observed at SVD.

Focal Mechanism and Seismic Moment

Because the Landers earthquake had such a large source dimension, the standard methods used to invert TERRAscope data for source parameters could not be applied. The focal mechanism and seismic moment were determined using teleseismic data collected soon after the earthquake by the IRIS Data Management Center. Here we only summarize the preliminary results, because the final results will be presented in another paper. The solution obtained by moment tensor inversion of long-period surface waves is: M_0=1.1x10^{27} dyne-cm (M_w=(logM_0/1.5)-10.7=7.3, Kanamori, 1978), dip=74°, rake=-176°, strike=340°. The seismic moments determined from surface waves and normal modes up to a period of 500 sec are essentially the same; no evidence for an increase in seismic moment at long period was found.

Inversion of teleseismic *P* and *S* waves using the method of Kikuchi and Kanamori (1991) revealed two distinct sub-events of 6 and 8 sec duration and about 10 sec apart, which are very well resolved in space and time. The source parameters for the first and second events are: M_0=1.9x10^{26} dyne-cm, dip=83°, rake=179°, strike=359°; and M_0=6.1x10^{26} dyne-cm, dip=87°, rake=178°, strike=333°, respectively. Both of these mechanisms show pure right-lateral strike-slip faulting. The change in strike from north to south along the fault is consistent with the distribution of aftershocks and the mapped surface break. The first focal mechanism is similar to the one obtained from the first-motion data (Hauksson *et al.*, 1992). In addition, the rupture pattern is in good agreement with directivity obtained from regional and teleseismic surface waves (Ammon *et al.*, 1992).

Magnitude, Radiated Energy and Stress Drop

The local magnitude, and the radiated energy were determined using the methods described by Kanamori *et al.* (1993). The average local magnitude determined from TERRAscope stations is M_L=6.81±0.39. The smaller value for M_L than for M_w is caused by saturation of the M_L scale.

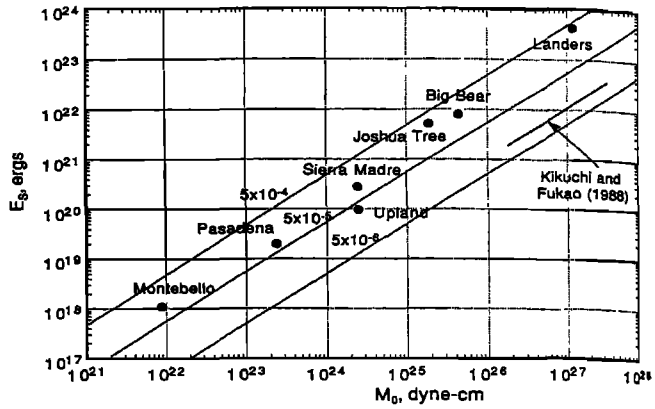

Fig. 2. The relation between the energy E_S and seismic moment M_0.

The radiated energy, E_S, of the Landers earthquake was determined to be 4.3x10^{23} ergs using TERRAscope data. For comparison, E_S estimated with Kikuchi and Fukao's (1988) method from the source time function determined from teleseismic data is 1.1 to 2.4x10^{23} ergs (Kikuchi, Written communication, 1992). The ratio E_S/M_0 is 3.9x10^{-4} (Figure 2), which is significantly larger than the average for large strike-slip earthquakes (Kikuchi and Fukao, 1988). This ratio which corresponds to a stress drop of 230 bars is comparable to the E_S/M_0 ratio of recent southern California earthquakes (1988 Pasadena, 1989 Montebello, 1990 Upland, 1991 Sierra Madre, 1992 Joshua Tree earthquakes, Kanamori *et al.* 1993). This suggests that the Landers earthquake belongs to the group of high stress drop earthquakes which, in light of the model of Kanamori and Allen (1986), occur on faults with a long recurrence time.

Directivity and Slip Distribution

The station PFO is located due south while the station GSC is located due north of the epicenter of the mainshock. The station PAS is located to the west of the mainshock epicenter or almost perpendicular to the rupture direction.

The displacement records from GSC, PFO, and PAS are shown in Figure 3. Although the epicenter is closer to PFO than to GSC, the maximum displacement at PFO is only 13 %

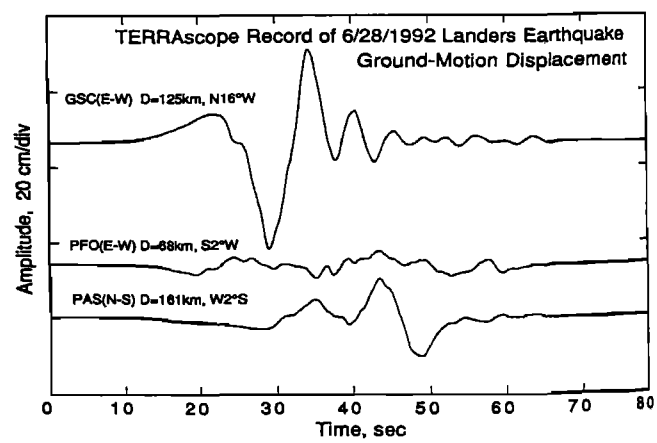

Fig. 3. Displacement records of the Landers earthquake recorded at TERRAscope stations GSC, PFO and PAS. Symbol *D* indicates the epicentral distance. The distances to GSC and PFO from the center of the rupture zone are about the same.

of that at GSC. Also, the signal is more spread out in time, or is more dominated by long periods, at PFO than at GSC. The difference reflects the directivity caused by the northward rupture propagation from the epicenter. When we corrected the TERRAscope data for directivity, the large amplitude asymmetry shown in Figure 3 could be eliminated. From the amplitude of TERRAscope data at periods of about 20 sec, the seismic moment is estimated to be 0.8×10^{27} dyne-cm, which is slightly smaller than that determined from long-period teleseismic waves.

The record obtained from PAS is intermediate between those from PFO and GSC in both amplitude and duration. To determine the rupture time history, we deconvolved the PAS record with the record of the M_w=4.3 foreshock (April 23, 1992, 02h25m30.1s GMT, 33.94° N, 116.33° W) of the 23 April 1992 Joshua Tree earthquake (M_w=6.1). The source parameters of this foreshock are: $M_0=3.1 \times 10^{22}$ dyne-cm, dip=70°, rake=176°, strike=345°. Because the epicenter and the focal mechanism of this earthquake are similar to those of the Landers earthquake, it can be used as an empirical Green's function for deconvolution.

The results of the deconvolution are shown in Figure 4. The first trace from the top is the Joshua Tree foreshock recorded at PAS. The second trace shows the moment-rate function. The peak value is given on the figure. The moment-rate function consists of two distinct pulses. This is consistent with the results from inversion of teleseismic body waves. The third trace is the convolution of the Joshua Tree foreshock and the moment-rate function. The fourth trace is the displacement record of the Landers earthquake obtained at PAS.

A similar deconvolution was done for the records from GSC and PFO, and the results are shown in Figure 5. The moment-rate function obtained from the PFO record has the two source pulses about 18 sec apart, as measured between the peaks. The moment-rate function obtained from the GSC record does not exhibit the double pulse structure, but consists of one triangular pulse with a duration of about 9 sec. This difference is consistent with the south-to-north directivity. The seismic moments estimated from the PAS, GSC, and PFO records are 0.9×10^{27}, 0.8×10^{27}, and 0.8×10^{27} dyne-cm, respectively, but these values depend on the estimate of seismic moment for the Joshua Tree foreshock, 3.1×10^{22} dyne-cm.

Since GSC and PFO are located on the extension of the

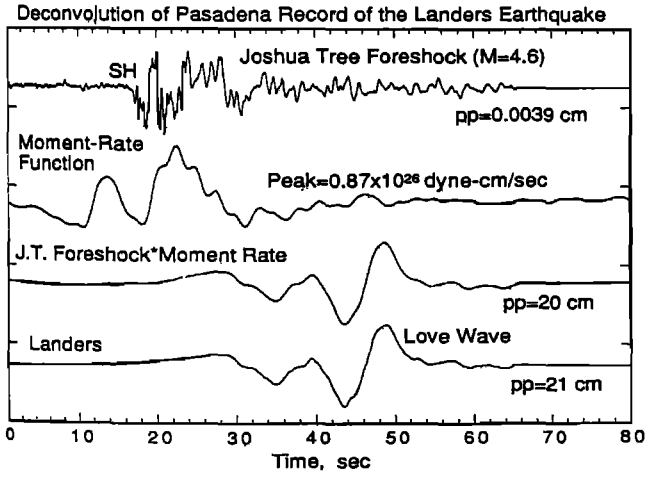

Fig. 4. The displacement record of the Landers earthquake (bottom) and the foreshock of the 23 April 1992 Joshua Tree earthquake (top trace) which is used for deconvolution of the Landers earthquake record. The second trace from the top is the moment-rate function obtained by deconvolution. The third trace from the top is the convolution of the Joshua Tree foreshock and the moment-rate function.

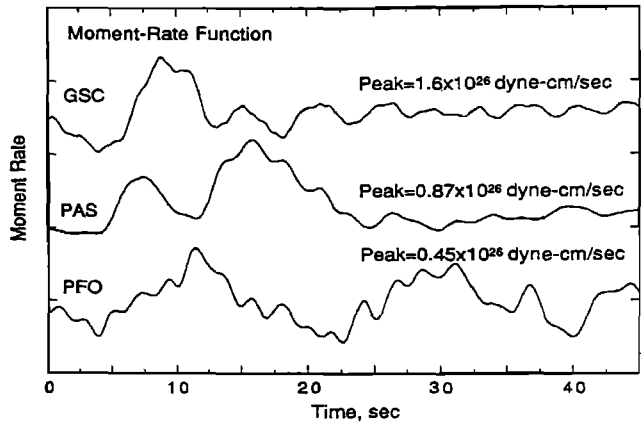

Fig. 5. Moment rate functions determined from the records of GSC, PAS and PFO.

fault, the distance from the rupture front varies significantly during rupture propagation, and the deconvolution for these stations is considered unreliable. In contrast, PAS is located in the direction normal to the rupture propagation so that the azimuth and the distance from the rupture front are essentially constant during rupture propagation. Thus the deconvolution result obtained from the Pasadena record is more reliable.

The moment-rate function obtained from PAS can be interpreted in terms of the slip distribution along the fault, though the interpretation presented here is not unique. Here, we interpret it using a modified Haskell (1964) model. For the Haskell model with spatially uniform dislocation over a fault with length L, constant local rise time, τ_0, and rupture velocity, V, the source moment-rate function is given by

$$M_0 \int_{-\infty}^{+\infty} r(t_1) s(\tau - t_1) dt_1 \qquad (1)$$

Here, M_0 is the seismic moment, and $s(t)$ is a box-car function with unit area and width τ_0. The function $r(t)$ is the "rupture function", which is a box-car function with unit area and width t_c. The time constant t_c is given by $L(1/V - \cos\Theta/c)$, where c is the apparent velocity of the wave considered, and Θ is the azimuthal angle between the station and the rupture direction. Equation (1) is a convolution of two box-car functions and gives a trapezoidal function.

If the dislocation is not uniform along the fault, we let $m(l)$ be the seismic moment per unit fault length, where l is the distance along the fault measured from the epicenter. Then equation (1) should be modified to

$$L \int_{-\infty}^{+\infty} m(t_1 L / t_c) r(t_1) s(\tau - t_1) dt_1 \qquad (2)$$

where $t_1 = l t_c / L$. If $\tau_0 \ll t_c$, then $s(t)$ can be approximated by a delta function, and equation (2)x(t_c/L), with $\tau L/t_c$ replaced by l, gives approximately the seismic moment per unit fault length. If the condition $\tau_0 \ll t_c$ does not hold, the moment distribution thus derived should be considered as a somewhat smoothed representation of the real moment distribution function.

For PAS, Θ=90° and $t_c = L/V$. We assumed that V=3 km/sec, the depth extent of fault W=15 km, and the rigidity of $\mu = 3 \times 10^{11}$ dyne/cm^2, and computed the slip distribution along the fault by $D(l) = m(l)/\mu W$, which is shown in Figure 6. The slip distribution function in Figure 6 indicates that the Landers earthquake consists of two distinct sub-events about 30 km apart, with the second event to the north being about twice as

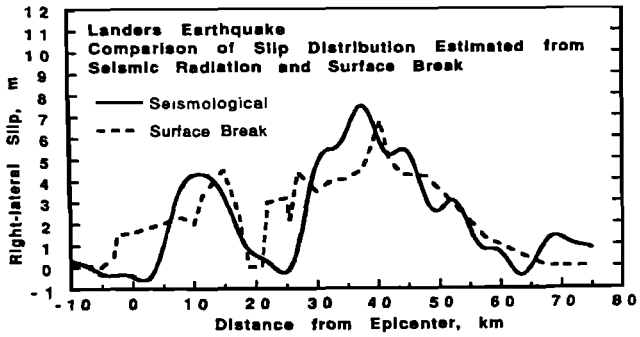

Fig. 6. The slip distribution along the fault estimated from the moment-rate function obtained from the TERRAscope record at PAS shown in Figure 4. A uniform rupture velocity of 3 km/sec, a depth extent of fault of 15 km and the rigidity of $3x10^{11}$ dyne/cm^2 are assumed. The dotted curve indicates the variation of surface break along the fault zone. All the surface breaks within ±2 km of the main rupture zone are projected on the line with a strike of N20°W (Hudnut, Written communication, 1992).

large as the first one. As shown in Figure 6, this distribution agrees very well with that determined from surface breaks (Landers Earthquake Response Team, 1992). This good agreement suggests that the assumption that the rise time of local dislocation is much shorter than the rupture time is correct.

Conclusions

Onscale strong-motion data recorded by TERRAscope in the near-field of the 1992 Landers earthquake have been used to estimate the magnitude, radiated energy, stress drop, source directivity and slip distribution of the mainshock. The strong directivity of seismic radiation to the north suggests that the rupture was mostly unilateral from Landers in the south toward Barstow in the north. Moment tensor inversion of long-period surface waves yielded a mechanism with M_0=1.1x10^{27} dyne-cm (M_w=7.3), dip=74°, rake=-176°, and strike=340°. Inversion of teleseismic P and S waves revealed two distinct sub-events of 6 and 8 sec duration and about 10 sec apart. The source parameters for the first and second events are: M_0=1.9x10^{26} dyne-cm, dip=83°, rake=179°, strike=359°; and M_0=6.1x10^{26} dyne-cm, dip=87°, rake=178°, strike=333°, respectively. The radiated wave energy, E_S, was estimated to be 4.3x10^{23} ergs. The ratio E_S/M_0=3.9x10^{-4} corresponds to a stress drop of 280 bars, and suggests long repeat times for the Landers fault system. The slip distribution extended over a distance of 60 to 70 km and showed two distinct peaks with a maximum of 4 and 7 m slip, respectively. A 2 to 4 km segment of fault between these peaks had almost no slip.

Near real-time availability of strong-motion parameters from TERRAscope is also very important for rapid hazard assessment in southern California. For instance, regions of high peak acceleration and velocity can be identified quickly.

Acknowledgements. Thorne Lay provided us with preliminary results of deconvolution of teleseismic data. Göran Ekström re-examined their moment tensor solution (CMT solution) upon our request. We thank Ken Hudnut for providing us with the figure for surface break. Reviews by David Boore and Ralph Archuleta were helpful in improving the paper. TERRAscope is mainly supported by grants from the L. K. Whittier Foundation and Arco Foundation. This research was partially supported by the U. S. Geological Survey Grant 14-08-0001-G1356. Contribution No. 5196, Division of Geological and Planetary Sciences, California Institute of Technology, Pasadena, California 91125. Southern California Earthquake Center Contribution No. 12.

References

Ammon, C. J., A. A. Velasco, and T. Lay, Rapid estimation of rupture directivity: Application to the 1992 Landers (M_S =7.4) and Cape Mendocino (M_S=7.2), California earthquakes, *Geophys. Res. Lett.*, submitted, 1992.

Haskell, N., Total energy and energy spectral density of elastic wave radiation from propagating faults, *Bull. Seismol. Soc. Am., 54*, 1811-1842, 1964.

Hauksson, E., L. Jones, T. Heaton, K. Hutton, J. Mori, S. Hough, H. Kanamori, and H.-K. Thio, The Landers and Big Bear earthquakes in Eastern San Bernardino County: June 28, 1992, *Preliminary Report of the Southern California Seismic Network, 6/28/1992*, 1992.

Joyner, W. B., and D. M. Boore, Peak horizontal acceleration and velocity from strong-motion records including records from the 1979 Imperial Valley, California, earthquake, *Bull. Seismol. Soc. Am., 71*, 2011-2038, 1981.

Kanamori, H., Quantification of earthquakes, *Nature, 271*, 411-414, 1978.

Kanamori, H., and C. R. Allen, Earthquake repeat time and average stress drop, in *Earthquake Source Mechanics*, vol. 6, edited by S. Das, J. Boatwright and C. H. Scholz, pp. 227, 1986.

Kanamori, H., E. Hauksson, and T. Heaton, TERRAscope and CUBE project at Caltech, *EOS, 72*, 564, 1991.

Kanamori, H., J. Mori, E. Hauksson, T. H. Heaton, L. K. Hutton, and L. M. Jones, Determination of earthquake energy release and M_L using TERRAscope, *Bull. Seismol. Soc. Am., 82*, in press, 1993.

Kikuchi, M., and Y. Fukao, Seismic wave energy inferred from long-period body wave inversion, *Bull. Seismol. Soc. Am., 78*, 1707-1724, 1988.

Kikuchi, M., and H. Kanamori, Inversion of complex body waves - III, *Bull. Seismol. Soc. Am., 81*, 2335-2350, 1991.

Landers Earthquake Response Team, L. E. R., Near-field Investigations of the Landers Earthquake Sequence, April-July, 1992, *Science, to be submitted*, 1992.

Doug Dreger, Egill Hauksson, Hiroo Kanamori, and Hong-Kie Thio, Seismological Laboratory, California Institute of Technology 252-21, Pasadena, CA 91125

Tom Heaton, U.S. Geological Survey, 525 S. Wilson Ave., Pasadena, CA 91106

(Received September 3, 1992;
accepted September 29, 1992)